A Complex Mechanism for Inducer Mediated Tau Polymerization†

Shaun W. Carlson, Mike Branden, Kellen Voss, Qian Sun, Carolyn A. Rankin, and T. Chris Gamblin*

Department of Molecular Biosciences, University of Kansas, Lawrence, Kansas 66045

Received February 27, 2007; Revised Manuscript Received May 19, 2007

ABSTRACT: The accumulation of polymers of the microtubule associated protein tau is correlative with increased neurodegeneration in Alzheimer's disease and other related tauopathies. In vitro models have been developed in order to investigate molecular mechanisms that regulate the polymerization of tau. Arachidonic acid and heparin have been proposed to induce tau polymerization via a ligand dependent nucleation−elongation mechanism. However, certain aspects of these in vitro results are inconsistent with a classic nucleation−elongation mechanism. Using steady state and kinetic analyses of tau polymerization at a variety of protein and inducer concentrations, we have found that the thermodynamic barrier for nucleation in the presence of inducers is negligible, which was manifested by increases in protein polymerization at low tau concentrations and very rapid kinetics of polymerization. However, the mechanism of polymerization is complicated by the observation that high concentrations of inducer molecules result in the inhibition of tau fibril formation through different mechanisms for arachidonic acid and heparin. These observations indicate that the molar ratio of inducer to protein is a greater determinant of the rate and extent of tau polymerization than the concentration of tau itself. Our results are therefore not consistent with a canonical nucleation−elongation reaction but rather are more consistent with an allosteric regulation model in which the presence of small molecules induce a conformational change in the protein that decreases the thermodynamic barrier for polymerization essentially to zero.

The microtubule-associated protein tau is a major component of the fibrillar structures that accumulate in neurofibrillary tangles, neuropil threads, and neuritic plaques in Alzheimer's disease (AD[1]). Filamentous deposits of tau can also be found in many other neurodegenerative tauopathies, such as Pick's disease, corticobasal degeneration, and progressive supranuclear palsy (reviewed in (*1*)). Because these deposits correlate with cognitive impairment and are not present in significant amounts in the normal brain, it is widely accepted that the formation of these filamentous structures is involved in the neurodegenerative process (reviewed in (*2*)). It is therefore of great importance to understand the molecular mechanisms that result in the abnormal polymerization of tau.

Inducer molecules, such as arachidonic acid (ARA), heparin, and other polyanionic compounds are used to drive rapid self-association of tau into fibrillar structures in vitro (reviewed in (*3*)). Although the physiological inducer of tau polymerization in AD is not known, the filamentous structures induced by ARA and heparin are structurally similar to those found in the disease (reviewed in (*4*)) and therefore serve as good models for pathological tau fibrillization. ARA induction of tau polymerization exhibits an apparent critical concentration for polymerization and proceeds via a partially folded thioflavine S-positive intermediate (reviewed in (*4*)). Heparin induced tau polymerization demonstrates a pronounced lag phase that can be reduced through the addition of nucleation seeds (*5*, *6*). The induction of tau polymerization has therefore been described to proceed via a ligand-dependent nucleation−elongation mechanism in which either ARA or heparin serves as the ligand (*5*−*9*).

Certain aspects of in vitro tau polymerization in the presence of inducer molecules are not consistent with a canonical nucleation−elongation mechanism. For example, the dose−response curves for the amount of polymerization with increasing tau concentrations are not linear (*9*, *10*), and some estimates for the critical concentration for polymerization are very close to zero (*8*, *11*). We now provide new evidence that demonstrates that tau polymerization in the presence of inducers is more complex than a simple nucleation−elongation mechanism. By altering the stoichiometry of inducers to protein, we have found that arachidonic acid and heparin reduce the energetic barrier for tau nucleation, resulting in increased polymerization at low protein concentrations. The amounts of polymer that could be detected under different conditions were dependent on the method of detection. Additionally, arachidonic acid and heparin inhibit polymerization at high inducer to protein ratios, resulting in structures similar in morphology to species previously described as intermediates in the polymerization process (*7*, *8*). These results are more consistent with an allosteric regulation of polymerization (*12*) with arachidonic acid and heparin acting as regulatory molecules or allosteric modifiers of the reaction.

These results are significant because they provide a new understanding of critical concentration as it relates to tau polymerization in the presence of inducer molecules. The

† Financial support was provided by NIH AG022428 (to T.C.G.).

* To whom correspondence should be addressed. Department of Molecular Biosciences, University of Kansas, 1200 Sunnyside Avenue, Lawrence, KS 66045. Tel: 785-864-5065. Fax: 785-864-5321. E-mail: gamblin@ku.edu.

[1] Abbreviations: AD, Alzheimer's disease; ARA, arachidonic acid; ThS, thioflavine S; LLS, laser light scattering.

10.1021/bi700403a CCC: $37.00
Published on Web 07/04/2007

stoichiometry of inducer molecules to protein concentration greatly influences the length and amount of filaments formed. The results also provide a potential explanation for the elusiveness of the physiological inducer of tau polymerization. Finally, the data presented provide evidence that the interaction of tau molecules with inducer molecules may provide a therapeutic target for blocking tau polymerization in disease.

EXPERIMENTAL PROCEDURES

Chemicals and Reagents. Arachidonic acid was obtained from Cayman Chemicals (Ann Arbor, MI), heparin sodium salt, grade I-A, from porcine intestinal mucosa lot 125K1336, and heparin sodium salt lot 116K1130 from Sigma (St. Louis, MO), IPTG from Calbiochem (EMD Biosciences, La Jolla, CA), thioflavine S from Sigma (St. Louis, MO), and uranyl acetate from Electron Microscopy Sciences (Fort Washington, PA). Tau protein (441 amino acids, corresponding to the longest central nervous system isoform) was expressed and purified as described previously (*13*). Protein concentration was determined by a commercial BCA assay from Pierce Chemical (Rockford, IL) using bovine serum albumin (Pierce Chemical, Rockford, IL) as a standard.

Polymerization Reactions in Vitro. Arachidonic Acid (ARA) induction: Tau protein (0−4 μM) in polymerization buffer (10 mM HEPES at pH 7.6, 100 mM NaCl, 0.1 mM EDTA, and 5 mM DTT) was incubated at room temperature in the presence of ARA (0−300 μM, concentration of ethanol carrier was kept constant at 3.75% for all reactions) for 6−20 h (*13*). Heparin induction: Tau protein (0−4 μM) in low-salt polymerization buffer (10 mM HEPES at pH 7.6, 15−40 mM NaCl, 0.1 mM EDTA, and 5 mM DTT) was incubated at 37 °C in the presence of heparin (0−6.25 μM) for 6−20 h (*14*). A polymerization reaction using a different source of heparin (Sigma 116K1130) gave virtually identical results to the heparin batch (Sigma 125K1336) used for the experiments in this manuscript (data not shown).

Thioflavine S fluorescence. Thioflavine S was added to tau polymerization reactions at a final concentration of 20 μM, and the resulting fluorescence was measured at λ_{ex} of 440 nm and λ_{em} of 520 nm in a 96-well-plate format in a Cary Eclipse fluorescence spectrophotomer (Varian Analytical Instuments, Walnut Creek, CA) (*13*).

Right Angle Laser Light Scattering. Tau polymerization reactions were placed into 5 × 5 mm fluorometer cuvettes (Starna Cells, Atascadero, CA) and illuminated with a 5 mW solid state 475 nm laser (B & W Tek, Inc., Newark, DE). Images of the resulting scattered light perpendicular to the incoming light were captured with a digital camera (Sony XC-ST270) and imported into Adobe Photoshop. The intensity of the scattered light was measured using the histogram feature of the software (*13*).

Transmission Electron Microscopy. Polymerization reactions were fixed at 1:10 (ARA) or 1:5 (heparin) dilutions with 2% glutaraldehyde, placed on Formvar-carbon coated grids, and stained with 2% uranyl acetate. Grids were viewed with a JEOL 1200 EXII electron microscope, and images were captured with the MegaViewII imaging system (Soft Imaging System, GmbH Münster, Germany). Filament lengths were extracted from digitized electron micrographs using the Optimas analytical imaging software (Media Cybernetics, Silver Spring, MD). Frequency distributions of filament lengths were generated by placing filaments into 50 nm bins with the center of the first bin at 25 nm. The number of filaments per bin was multiplied by the bin center to generate the approximate mass of filaments within a given length of filaments. The mass per bin was then divided by the total filament mass to give a percent of total mass for each range of filament lengths (*13*).

Kinetics of Polymerization. The kinetics of tau polymerization reactions at protein concentrations from 0.5 to 4.0 μM in the presence of optimal, limiting, and inhibitory ratios of ARA and heparin were followed by fluorescence in the presence 20 μM ThS using a FlexStation II fluorometer microplate reader (Molecular Devices Corporation, Sunnyvale, CA). The data were fit to a single phase exponential association equation using GraphPad Prism software. The data for optimal ratios of ARA were fit using a mathematical model developed for the kinetics of actin nucleation and polymerization (*25*) by first fitting the 4 μM tau curve for values of n, k^+, and K_{n-1} and then using these values to fit the data from the other protein concentrations.

Determination of Monomer Concentrations at Apparent Steady State. The amount of tau monomer in solution following a polymerization reaction was determined using a centrifugation assay (*15*). Tau polymerization reactions were performed with either heparin or ARA for approximately 20 h using the conditions listed above and then overlaid onto a 40% glycerol cushion and centrifuged at 80,000 rpm in a Beckman TLA-100 rotor for 20 min at 26 °C (*15*). The samples from the upper layer were analyzed by SDS−PAGE using the Bio-Rad Silver Stain Plus Kit (Hercules, CA). Band intensities were estimated in Adobe Photoshop and the concentration of monomer in the upper layer was calculated from a tau standard curve in the same gel using GraphPad Prism software. The depletion of filaments from the upper layer was confirmed by electron microscopy (data not shown).

Determination of Ligand Binding to Tau Filaments. Tau polymerization reactions ranging from 2−4 μM total protein were performed with either H^3-labeled heparin (0.376 μM) or ARA (75 μM) for approximately 20 h using the conditions listed above and then centrifuged at 80,000 rpm in a Beckman TLA-100 rotor for 30 min at 26 °C. The supernatants were removed, and the pellet was resuspended in 5% SDS in 0.1 M NaOH (*16*). The amount of radioactivity in the supernatants and pellets was measured with a Packard 1600TR liquid scintillation counter. The concentration of protein in the pellet was determined using a BCA protein assay. The centrifugation tubes used for ARA were siliconized before use in an effort to reduce the amount of ARA background. The pellets were not washed because significant amounts of radioactivity were lost for each of three washes performed with assembly buffer. The amount of radioactivity in the supernatants and pellets following the centrifugation of an assembly incompetent form of tau (I277,208P) (*17*, *18*) served as a control for background binding and was subtracted from the values for wild type tau.

RESULTS

Efficient Tau Polymerization Requires Inducer Molecules. Several concentrations of full length tau protein were

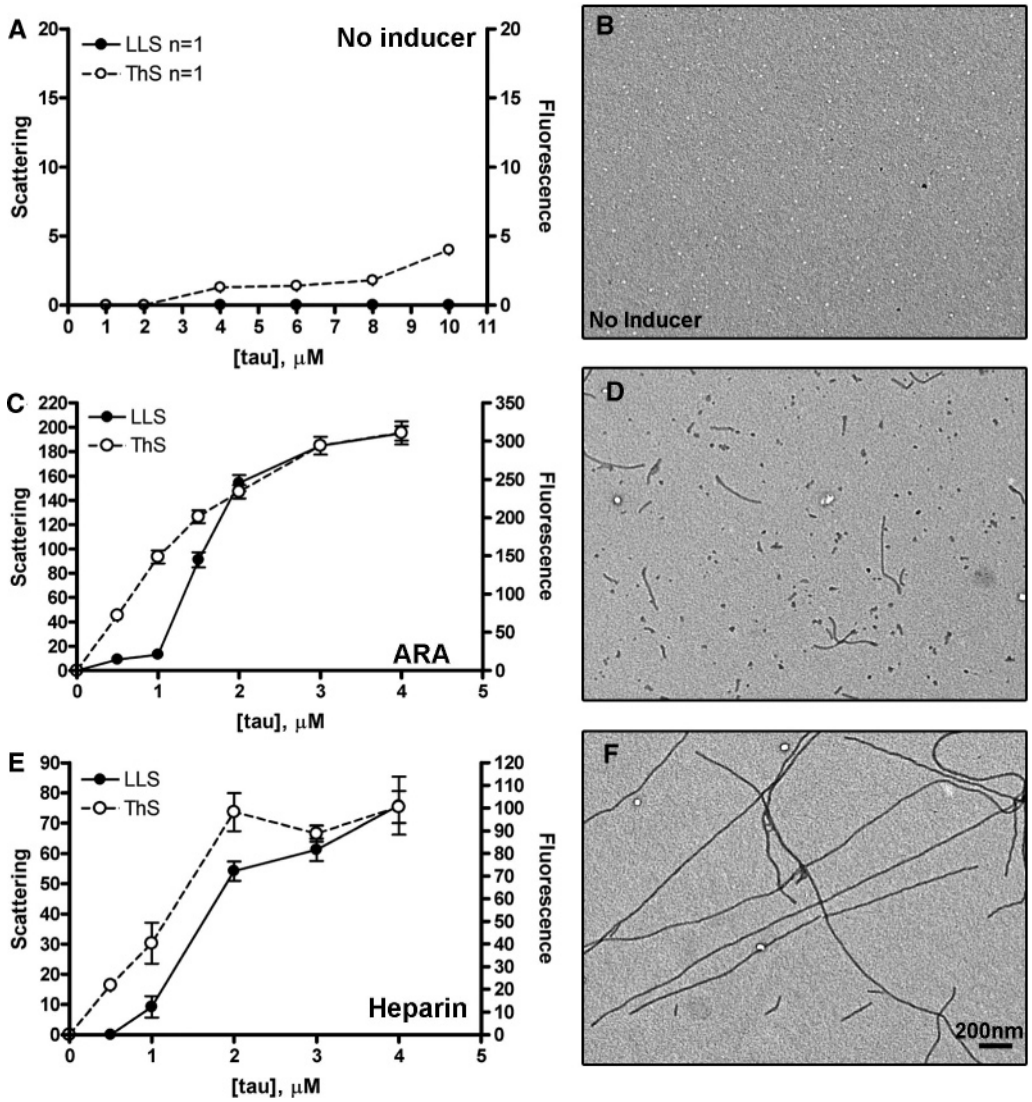

FIGURE 1: Nonlinearity of tau polymerization with regulatory molecules. Tau protein at various concentrations (*x*-axis) was incubated alone (A and B), with 75 μM ARA (C and D), and with 0.376 μM heparin (E and F) for approximately 16 h, and the final extent of polymerization was determined by LLS (●, left *y*-axis) and ThS fluorescence (○, right *y*-axis). The presence or absence of filaments was confirmed by EM (B, D, and F). Note that the scales of the *x*-axes and *y*-axes are different for the different conditions because virtually no polymerization was observed without regulatory molecules, and ARA gave a much stronger signal than did heparin under these conditions. Data in A represent a single experiment. C and E show an average of three experiments ± SEM. The scale bar in F represents 200 nm and applies to each micrograph.

incubated for approximately 20 h either alone or in the presence of 75 μM arachidonic acid (ARA) or 0.376 μM heparin (Figure 1). Levels of polymerized tau were monitored by thioflavine S (ThS) fluorescence, laser light scattering (LLS) and electron microscopy (EM). Consistent with previously published results (*19*), no polymer could be detected by any of the three methods when tau was incubated without inducer (Figure 1A and B). High levels of polymerized tau were detected by all three methods in the presence of 75 μM ARA (Figure 1C and D). However, the dose−response curves for the amount of polymer detected by ThS consistently gave a different shape than was detected by LLS, especially at low protein concentrations (Figure 1C). Furthermore, the levels of measured polymer were not linear over the entire protein concentration range for LLS and ThS (Figure 1C). In the presence of 0.376 μM heparin (Figure 1E and F), products of polymerization were detected by all three methods, although the dose−response curves for ThS and LLS did not appear to agree at low protein concentrations. As was observed for the ARA inducer, in the presence of a constant concentration of heparin inducer, the amount of polymer formed was not linear over the entire range of protein concentrations when using LLS and ThS as detection methods (Figure 1E).

To determine the theoretical lowest concentration of protein required for polymerization in the presence of inducers, the amount of tau polymer observed at differing total protein concentrations in the presence of inducer molecules can be fit to a linear regression (*7*, *11*, *20*−*22*). The *x*-intercept is commonly referred to as the critical concentration for polymerization. These values were determined by fitting the linearly increasing part of the curves for LLS using linear regression analysis. For the ARA reactions (Figure 1C), the *x*-intercept (fitting the final polymer amounts at 1−2 μM total protein) was 0.9 μM. For heparin (Figure 1E), the *x*-intercept (fitting the final polymer amounts at 0.5−2 μM total protein) was 0.6 μM. The predicted *x*-intercept for polymerization as determined by

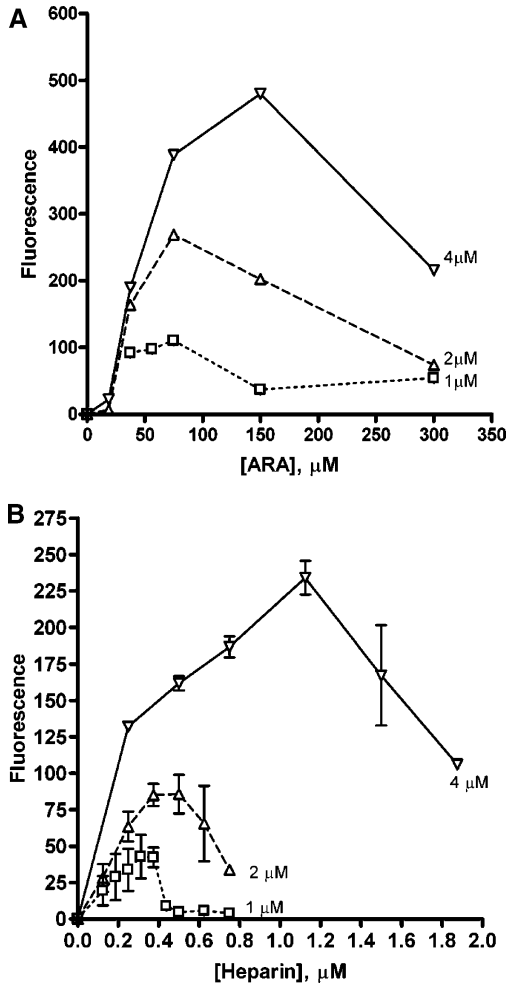

FIGURE 2: Variation of regulatory molecule concentrations in tau polymerization reactions. Tau polymerization reactions at 1 (□), 2 (△), and 4 (▽) μM protein concentration were mixed with various concentrations of (A) ARA or (B) heparin and incubated for approximately 20 h. ThS was added at a final concentration of 20 μM, and the amount of resulting fluorescence was determined. The error bars denote the SEM.

ThS fluorescence was zero for both ARA and heparin (Figure 1C and E).

Concentration of Inducer Molecules Determines the Extent of Tau Polymerization. In the above experiments, the concentrations of inducer molecules are held constant as the protein concentration is varied. We hypothesized that the observed nonlinearity at high protein concentrations was due to limiting amounts of inducer. Tau polymerization reactions were therefore performed at several different concentrations of inducers. The resulting dose−response curves were not linear but biphasic. The amount of polymer detected by ThS fluorescence increased to a peak, then declined (Figure 2A and B). Similar results were obtained using LLS as a detection method (data not shown). At each of the three protein concentrations tested, the maximum ThS fluorescence was reached at approximately the same stoichiometry of inducer to protein. For ARA, this ratio was 37.5 to 1 of inducer to protein. For heparin, this ratio was 0.188 to 1 of inducer to protein. These results indicate that there is an optimal ratio of inducer to protein. Below this ratio, the concentration of inducer limits the reaction, and above this ratio, the concentration of inducer inhibits the reaction. For example, at 4 μM protein and 75 μM ARA, the concentration of the inducer is limiting because the amount of polymer increases when the ARA concentration is increased to 150 μM. Increasing the inducer concentration further to 300 μM is inhibitory because the amount of polymer is less than that observed with 150 μM. This effect explains the observed nonlinearity in tau polymerization reactions when the tau concentration was increased while the concentrations of the inducer were held constant (Figure 1).

Constant Molar Ratios of ARA to Protein Result in Linear Increases in Polymer Formation. Because increases or decreases in the molar ratio of inducer to protein resulted in nonlinear amounts of tau polymerization, we hypothesized that maintaining a constant molar ratio would ameliorate these effects. Therefore, polymerization reactions were performed at varying protein concentrations while maintaining a constant molar ratio of ARA to protein. Linear increases in polymer were observed for limiting (18.75:1), optimal (37.5:1), and inhibitory (75:1) ratios of ARA (Figure 3). The amount of tau polymer detected by LLS and ThS using the limiting and optimal ratios of ARA to protein showed high correlation, whereas there was less correlation between the two methods using the inhibitory ratio. The data in Figure 3 was fit by linear regression in order to determine the *x*-intercept, which should represent the predicted lowest protein concentration required for tau polymerization (Table 1). The *x*-intercepts for the three molar ratios of ARA to protein were not the same. The inhibitory ratio resulted in a lower value for the *x*-intercept than that at optimal conditions, and the limiting ratio resulted in a higher value for the *x*-intercept than that at optimal conditions.

Molar Ratio of ARA to Protein Determines the Number and Length of Filaments. Changes in filament length or morphology could greatly alter the amount of scattered light (*23*) and the degree of ThS binding to filaments (*24*). We hypothesized that changes in filament length or morphology could be responsible for the discrepancy in the ThS and LLS measurements under inhibitory conditions. The use of inhibitory polymerization conditions, that is, low protein and high ARA concentrations, resulted in the majority of the filament mass belonging to filaments shorter than 50 nm in length (Figure 4A and B). The mass of filaments formed under optimal and limiting conditions was more evenly distributed among all filament lengths, due mainly to an increase in the number of longer filament species (Figure 4C−E). These results indicate that filament length and morphology impact the ability to detect tau filament formation using the LLS and ThS techniques and that filament length and morphology are dependent on the inducer/tau stoichiometry.

Because the length and morphology of the filaments changed as a function of protein concentration at constant ARA concentrations, we hypothesized that maintaining a constant stoichiometry between ARA and tau would result in more similar filament morphologies. The average length, number, and mass of filaments formed at a constant ARA concentration were plotted against total protein concentration and compared to three protein concentrations where the optimal molar ratio was maintained (Figure 5A−C).

In the presence of a fixed concentration of ARA, the average filament length varied with changing protein concentrations. However, when the stoichiometry of ARA to protein was kept constant, the average filament lengths were

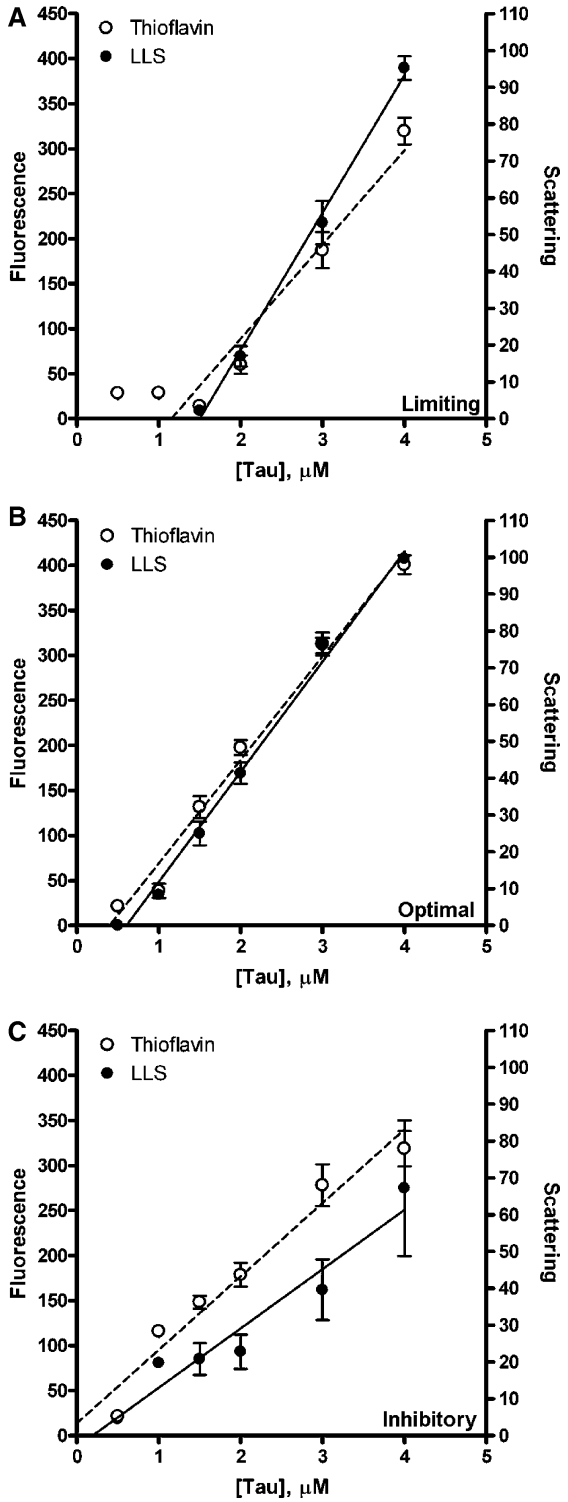

FIGURE 3: Polymerization of tau in the presence of different molar ratios of ARA. Tau polymerization reactions were performed at various protein concentrations (0.5−4.0 μM, *x*-axis) for approximately 16 h. The concentration of ARA was varied along with the concentration of protein to maintain (A) a limiting (18.75:1) molar ratio, (B) an optimal (37.5:1) molar ratio, and (C) an inhibitory (75:1) molar ratio of inducer to protein at each protein concentration. The samples were measured using LLS (●, right *y*-axis) and ThS (○, left *y*-axis). The error bars represent the SEM. The lines represent the linear regression analysis of the data to obtain apparent critical concentrations for the polymerization for Ths (---) and LLS (—).

similar to each other at all protein concentrations tested (Figure 5A). Both the number and overall mass of filaments formed in the presence of a constant molar ratio of ARA increased in a linear fashion with increasing protein concentration (Figure 5B and C). There was no linear relationship between the number of filaments and increasing protein concentration with the fixed inducer concentration (Figure 5B). The mass of filaments formed with the fixed inducer concentration increased with a different slope than that of the constant molar ratio (Figure 5C). These results confirm that maintaining constant molar ratios of ARA with increasing protein concentrations results in filament populations with similar lengths.

Table 1: Predicted Lowest Concentration Required for Tau Polymerization in the Presence of Constant Stoichiometries of Inducer Molecules[a]

	arachidonic acid			heparin		
	ThS	LLS	*n*	ThS	LLS	*n*
limiting	1.45 ± 0.10	1.51 ± 0.10	4	0.09 ± 0.04	0.41 ± 0.06	4
optimal	0.40 ± 0.11	0.60 ± 0.10	3	0.26 ± 0.04	0.47 ± 0.05	4
inhibitory	−0.20 ± 0.18	−0.07 ± 0.51	5	0.56 ± 0.27	0.75 ± 0.34	4

[a] All concentration values are in μM ± SD.

Kinetics of ARA Induced Tau Polymerization. Because the kinetics of a polymerization reaction can shed light on the mechanism of polymerization, the increase in polymer formation was monitored over time using ThS fluorescence at different protein concentrations with optimal, limiting, and inhibitory ratios of ARA (Figure 6). The resulting polymerization curves were fit by a simple one phase exponential association equation

$$Y = Y_{max}(1\text{-}e^{(-Kt)}) \quad (1)$$

where the amount of polymer increases from zero to Y_{max} with the rate constant K. The half time of the reaction is $0.69/K$. In each case, the half polymerization time, $t_{1/2}$, was similar for all protein concentrations at a given ARA/tau ratio (Figure 6E). The values for K were also similar for all protein concentrations at a given ARA/tau ratio (Figure 6F). However, K and $t_{1/2}$ were not the same for all ARA/tau ratios. The inhibitory conditions had a significant reduction in $t_{1/2}$ ($P < 0.0001$) than that at optimal and limiting conditions, which were not significantly different ($P = 0.1432$). This information, when combined with the observation that inhibitory conditions give more but shorter filaments than optimal and limiting conditions, would suggest that the mechanism for inhibition of elongation is through a great increase in nucleation to the point that there are too few monomers to participate in the elongation phase.

Kinetic analysis can also give information as to the size of the nucleus of the polymerization reaction because $t_{1/2}$ at different protein concentrations should be inversely proportional to the $(n/2)$-power of the total protein concentration (where n is equal to the size of the nucleus) (*12*). However, this analysis does not apply under these conditions because $t_{1/2}$ does not vary with protein concentration at constant molar ratios of inducers. In fact, we attempted to fit our kinetic analysis to a more rigorous mathematical model developed for the kinetics of action nucleation and polymerization (*25*):

$$\frac{dT_f}{dt} = k^+C(T_1 - T_1^\infty) \quad (2)$$

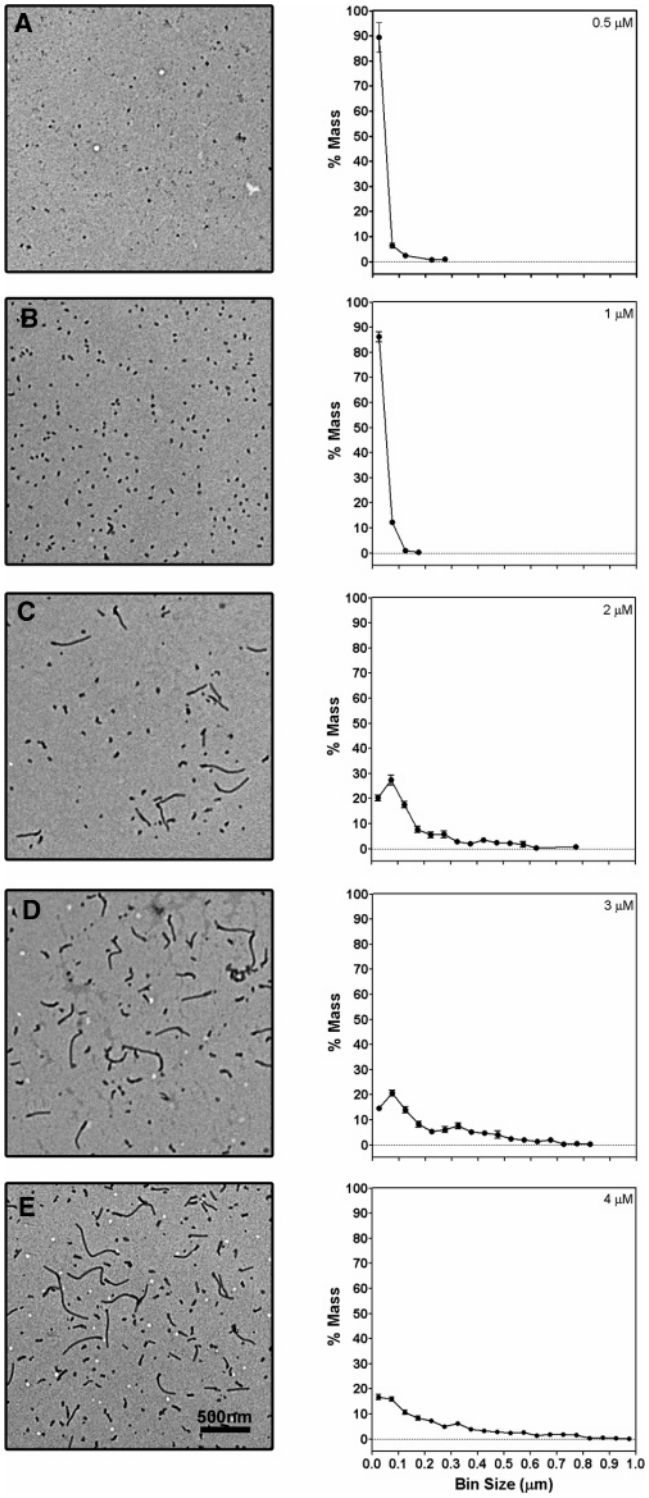

FIGURE 4: Length distribution of tau filaments changes as a function of protein concentration. Representative electron micrographs taken at 20,000× (the bar in E represents 500 nm and is applicable to all images) for polymerization reactions in the presence of 75 μM ARA following approximately 16 h of polymerization are shown for several different concentrations of tau: (A) 0.5 μM; (B) 1.0 μM; (C) 2.0 μM; (D) 3.0 μM; and (E) 4.0 μM. The average mass frequency distributions are shown for each of these concentrations and are plotted as the percent of the total mass that one bin represents (*y*-axis) vs the center of the bin size (*x*-axis).

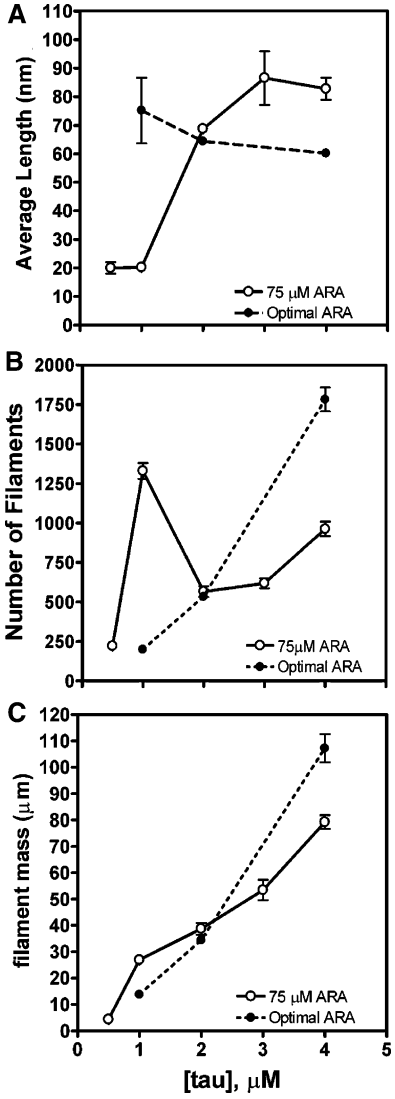

FIGURE 5: Effect of ARA inducer concentration on tau filament morphology. Tau polymerization reactions were performed at 0.5, 1, 2, 3, and 4 μM in the presence of a constant 75 μM ARA (○). Tau polymerization reactions at 1, 2, and 4 μM were also performed with an optimal (37.5:1) ratio ARA/tau (●). Reactions were viewed by electron microscopy. (A) The average of the average filament lengths from 5 fields. (B) The average number of filaments for these same five fields. (C) The filament mass or the total length of filaments measured is depicted. Error bars represent the SEM.

where T_f is the concentration of tau filaments, T_1 is the concentration of tau monomers, T_1^∞ is the concentration of monomer at apparent steady state (critical concentration), k^+ is the rate constant for the addition of monomer at the ends of the filaments, and C is the concentration of polymer addition sites. The nucleation rate is calculated by the following equation:

$$\frac{dC}{dt} = K_{n-1}k^+(T_1)^{n-1}(T_1 - T_1^\infty) \quad (3)$$

where K_{n-1} is the association constant for the formation of nuclei, and n is equal to the size of the nucleus. Although any particular concentration of protein can be fit by several combinations of K_{n-1}, k^+, and n, there should only be one solution for n that allows all protein concentrations to be fit simultaneously (*25*). In our case, assuming that the *x*-intercept to a linear regression of the final extent of polymerization was equal to T_1^∞, and assuming that the amount of ThS fluorescence at apparent steady state was equal to the concentration of polymer (calculated by subtracting the critical concentration from the total concentration), the size

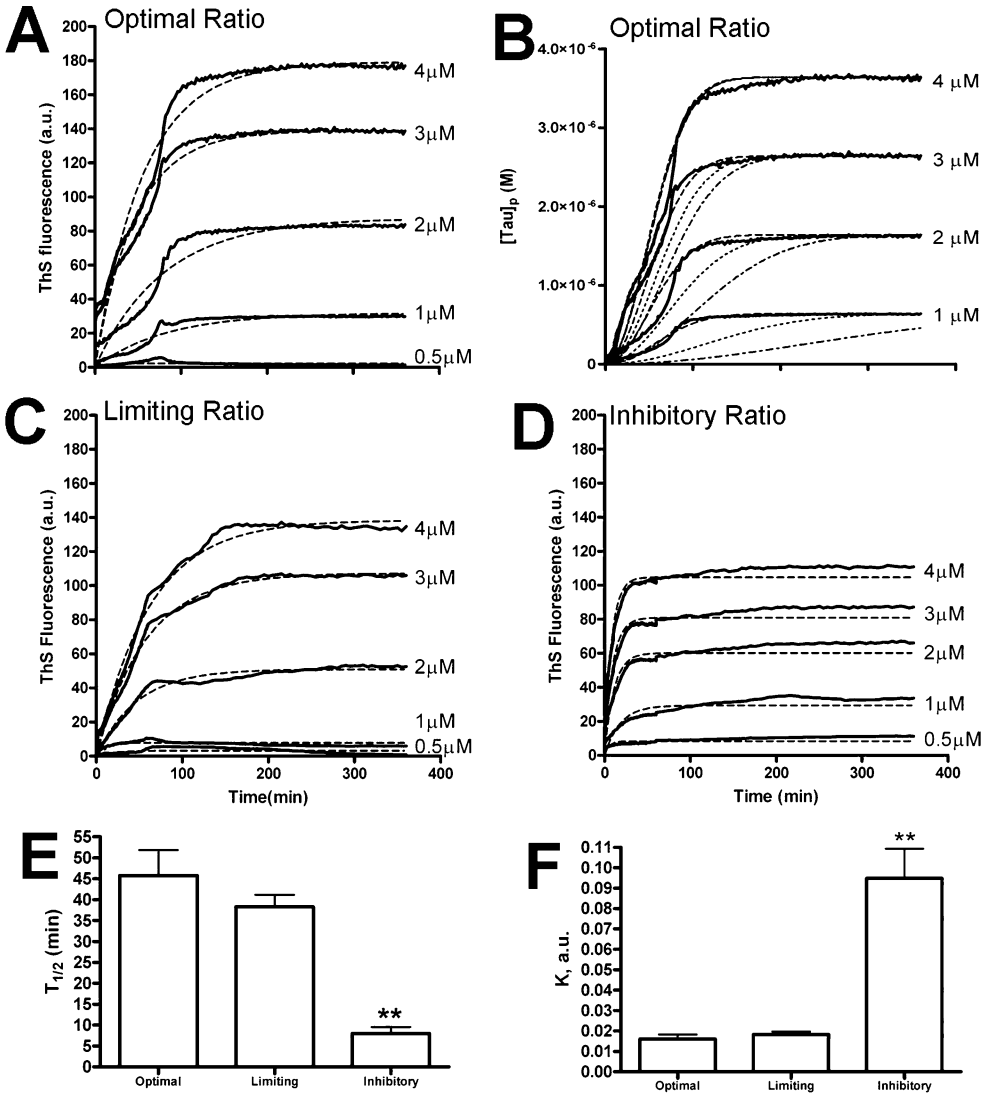

FIGURE 6: Kinetics of ARA induction of tau polymerization. The kinetics of tau polymerization was followed with ThS fluorescence at a constant molar ratio of (A) 37.5:1 (Optimal), (B) 37.5:1 (Optimal), (C) 18.75:1 (Limiting), and (D) 75:1 (Inhibitory) at 0.5, 1, 2, 3, and 4 μM tau ((—), individually labeled on graph). The data in A, C, and D were fit to a single phase exponential association equation to obtain the values for (E) $t_{1/2}$ and (F) K. The data in E and F are the average values ± SEM for all polymerization reactions that had final polymerization values of more than 10 ThS units. The asterisks denote values that were significantly different from optimal conditions. The data in B was converted to molar concentrations of tau using the assumptions listed in the Results and fit to equations derived for the kinetics of actin nucleation and polymerization (*25*) using $n = 0$, $k^+K_{nuc} = 5 \times 10^{-4}$ s^{-2} M^{-4} (---), $n = 1$, $k^+K_{nuc} = 1.2 \times 10^2$ s^{-2} M^{-4} (••••), and $n = 2$, $k^+K_{nuc} = 3 \times 10^7$ s^{-2}M^{-4} (•-•-).

of the nucleus that allowed all protein concentrations under optimal inducer conditions to be fit by the same parameters for K_{n-1} and k^+ was zero (Figure 6B).

Constant Molar Ratios of Heparin to Protein Result in Linear Increases in Polymer Formation. Similar results were obtained using heparin as a regulatory molecule to induce tau polymerization (Figure 7). Each of the three inducer to protein ratios (limiting, optimal, and inhibitory) gave linear dose−response curves unlike the curves observed with constant concentrations of inducer (compare with Figure 1C). Each inducer to protein ratio tested had a different *x*-intercept value as determined by linear regression analysis of the ThS and LLS data. In stark contrast to the results with ARA, the limiting ratio *x*-axis intercept was lower than that of the optimal ratio, whereas the inhibitory ratio resulted in a higher *x*-axis intercept for the theoretical protein concentration required for polymerization (Table 1). These important results highlight that there are differences between the modes of ARA and heparin induction of tau polymerization. Nevertheless, the variation of the stoichiometry of both inducers to protein affect the theoretical protein concentration required for tau filament formation.

Kinetics of Heparin Induced Tau Polymerization. The polymerization of tau in the presence of heparin was monitored over time using ThS fluorescence (Figure 8A−C). In the presence of optimal, limiting, and inhibitory ratios of heparin, the estimate for $t_{1/2}$ by fitting to eq 1 was very similar at the different protein concentrations. The rate of polymerization estimated by $t_{1/2}$ was similar for optimal and limiting conditions, but unlike ARA, the $t_{1/2}$ for the inhibitory conditions was actually increased compared to that at optimal and limiting conditions (Figure 8D). When comparing the estimated rate constants, limiting conditions had a lower value for K, and the inhibitory condition was lower still (Figure 8E). The kinetics of polymerization was much slower than that observed with ARA (compare with Figure 6). This

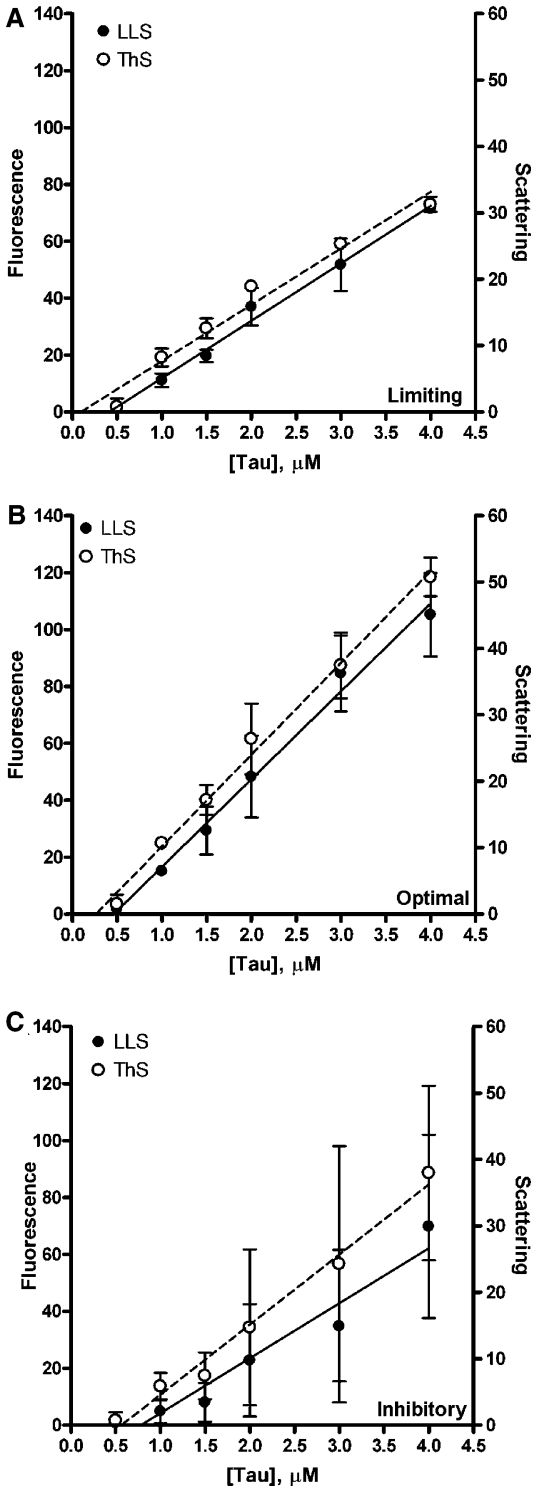

FIGURE 7: Polymerization of tau in the presence of different ratios of heparin. Tau polymerization reactions were performed at various protein concentrations (0.5−4.0 μM, *x*-axis) for approximately 16 h. The concentration of heparin was varied along with the concentration of protein to maintain (A) a limiting (0.094:1) molar ratio, (B) an optimal (0.188:1) molar ratio, and (C) an inhibitory (0.282:1) molar ratio of heparin to protein at each protein concentration. The samples were measured using LLS (●, right *y*-axis) and ThS (○, left *y*-axis). The error bars represent the SEM. The lines represent the linear regression analysis of the data to obtain apparent critical concentrations for the polymerization for ThS (---) and LLS (—).

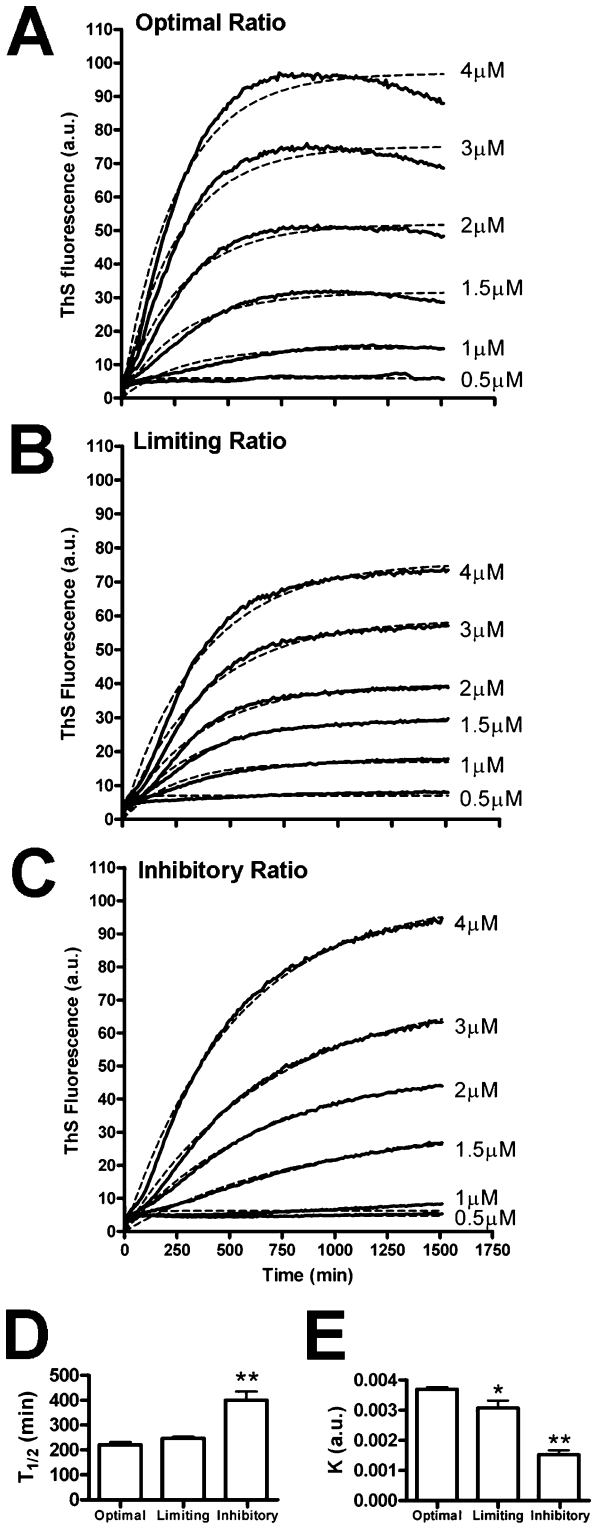

FIGURE 8: Kinetics of heparin induction of tau polymerization. The kinetics of tau polymerization was followed with ThS fluorescence at a constant molar ratio of (A) 0.188:1, (B) 0.094:1, and (C) 0.376:1 at 0.5, 1, 1.5, 2, 3, and 4 μM tau ((—), individually labeled on graph). The data were fit to a single phase exponential association equation to obtain the values for (D) $t_{1/2}$ and (E) *K*. The data in D and E are the average values ± SEM for all polymerization reactions that had final polymerization values of more than 10 ThS units. The asterisks denote values that were significantly different from those at optimal conditions.

result, combined with the differences observed in filament morphology strongly suggests that heparin is not as efficient for the nucleation of tau polymerization. However, because the $t_{1/2}$ did not show an inversely proportional relationship to the total protein concentration, this reaction still cannot

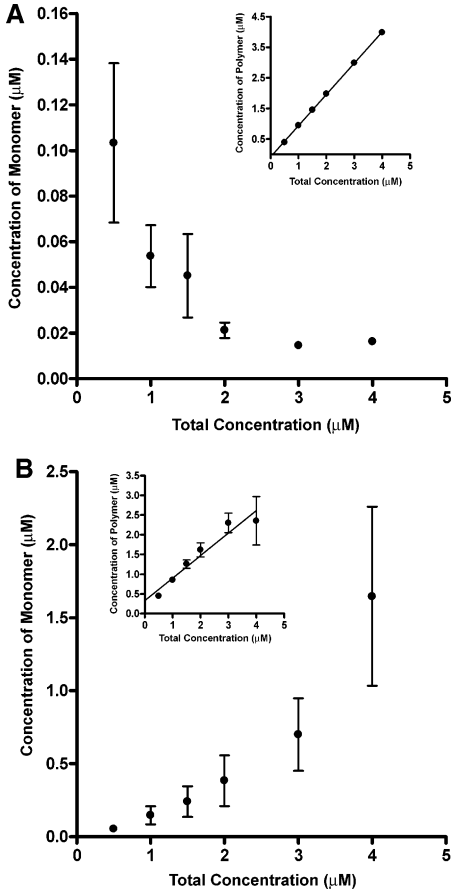

FIGURE 9: Centrifugal analysis of monomer concentration following polymerization. The monomer remaining in solution following polymerization reactions at various tau protein concentrations and (A) an optimal (37.5:1) molar ratio of ARA or (B) an optimal (0.188:1) molar ratio of heparin was separated from polymer via centrifugation. The resulting samples were analyzed by silver stained SDS−PAGE using non-polymerized tau as a standard. The band intensities of the monomeric protein remaining after centrifugation were converted to concentrations (*y*-axis) and plotted against total protein concentration in the reaction (*x*-axis). The concentration of polymer was calculated by subtracting the concentration of monomer from the total concentration. The concentration of polymer (*y*-axis) was then plotted against total concentration (*x*-axis) in the insets in A and B. The data presented are the averages of three independent trials ± SEM.

be considered to be a canonical nucleation−elongation reaction.

At Apparent Steady State, the Concentration of Unpolymerized Monomer Does Not Remain Constant with Varying Protein Concentrations. To further test the amount of polymerization observed in the presence of inducers, a centrifugation assay was performed to determine the concentration of unpolymerized tau remaining at apparent steady state. The optimal ratios of protein and regulatory molecules were employed to avoid the complication of limiting or inhibitory conditions. The monomer was separated from the polymer by ultracentrifugation over a 40% glycerol cushion. The concentration of monomer remaining was determined by silver stained SDS−PAGE (Figure 9). The concentration of monomer was not constant with increasing total protein concentration in the presence of ARA but rather decreased with increasing total protein concentration (Figure 9A). When the concentration of polymerized of tau was calculated from this data by subtracting the concentration of monomer from the total amount of protein (Figure 9A, inset), the dose−response curve was similar to those observed for LLS and ThS (compare with Figure 3B). The *x*-axis intercept to a linear regression of the data for polymerization was 0.08 ± 0.05 μM in the presence of ARA. The concentration of monomer remaining in solution following heparin induced polymerization reactions increased with increasing protein concentrations (Figure 9B). The plot of the concentration of polymer versus total protein concentration was linear and had an *x*-axis intercept to a linear regression of −0.80 ± 0.70 μM (Figure 9B, inset). The most important observation from this data is that in both cases the concentration of unpolymerized monomer was not constant as the protein concentration increased in the presence of a constant optimal molar ratio of inducer to protein. These data call into question the currently accepted model that the *x*-axis intercept of tau represents the critical concentration for polymerization. Instead, our data indicate that tau polymerization in the presence of inducers does not have a true critical concentration for polymerization.

Binding of ARA and Heparin to Tau. In order to better understand the mechanism for ARA and heparin induction of tau polymerization, the degree of binding of ARA and heparin to tau filaments was measured using radiolabeled ligands in a centrifugal assay (*16*, *26*). As seen in Figure 10A, no significant binding of ARA above background levels could be detected. Heparin binding above background could be detected, but the degree of binding was very low (approximately 1 mol heparin bound per 20 mol of polymerized tau) (Figure 10B). These low levels of binding have been interpreted in the literature as indicating that ARA and heparin are not incorporated into the core of the filament (*16*, *26*).

DISCUSSION

For any protein polymerization system, it is of fundamental importance to understand the molecular mechanisms that regulate the process. This is especially true of tau polymerization because the formation of neurofibrillary tangles has been correlated to neurodegeneration. The disruption of tau polymerization could therefore be a therapeutic target for Alzheimer's disease and other related dementias.

Tau Has a High Energetic Barrier for Polymerization. In the absence of inducer molecules, tau exhibits a very high critical concentration for polymerization, both in vitro (*4*) and in vivo (*27*), owing to its high solubility and high degree of disorder (*6*, *10*). Our results confirm this observation, with no tau polymerization observed at concentrations as high as 10 μM in a 20 h period (Figure 1). Because no spontaneous nucleation is observed at these concentrations, tau polymerization is very likely more complex than a simple linear polymerization process. Because the rate-limiting step appears to be nucleation, tau polymerization has been hypothesized to proceed via a nucleation−elongation mechanism (*4*−*9*).

Inducers Lower the Energetic Barrier of Tau Polymerization. The polymerization of tau can be enhanced in vitro through the addition of inducer molecules such as arachidonic acid (ARA) or heparin (reviewed in (*3*)). Our results agree with these studies, showing that the concentration of tau required for polymerization is decreased in the presence of

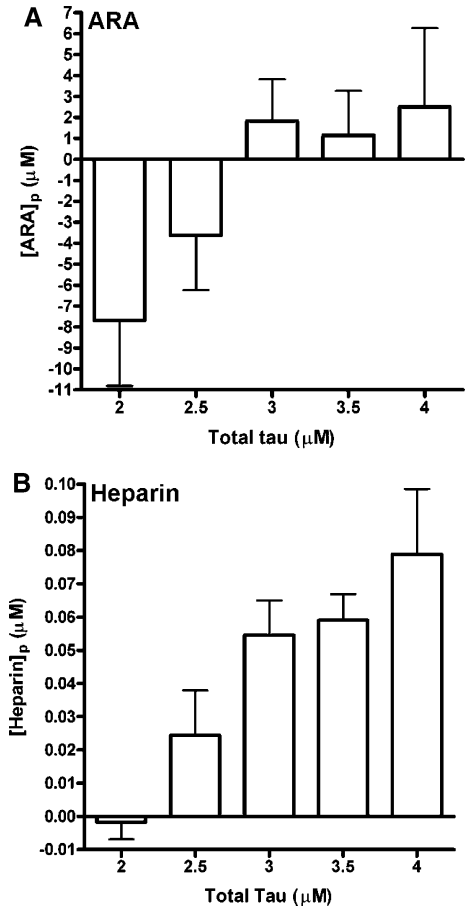

FIGURE 10: Binding of ARA and heparin to tau filaments. The amount of radiolabeled ligand that co-sedimented with tau filaments following centrifugation was determined for (A) 75 μM ARA and (B) 0.376 μM heparin in the presence of various concentrations of tau. The amount of radiolabeled ligand that was detected following the centrifugation of an assembly incompetent form of tau (I277,-308P) was subtracted from the values. The data represent three independent trials ± SEM.

ARA and heparin (Figure 1). The addition of inducers, therefore, reduces the energetic barrier for polymerization. However, the mechanism for tau polymerization in the presence of inducers is not consistent with a canonical nucleation−elongation model.

Tau Does Not Exhibit a True Critical Concentration for Polymerization in the Presence of Inducer Molecules. A major feature of a nucleation−elongation mechanism for polymerization is a critical concentration for polymerization, that is, a concentration of protein below which no polymerization is observed because of the thermodynamic barrier of nucleation. In the presence of inducers, this predicted concentration is zero under several polymerization conditions. The apparent critical concentration observed under other conditions can be different depending on the method chosen for detecting tau polymerization and the concentration of inducer molecules (Table 1), indicating that these values are most likely the limit of detection of polymerization for that particular method. The concentration of monomer remaining in a reaction following polymerization is not constant, preventing the designation of a critical concentration (Figure 9). Although the critical concentration of tau polymerization in the presence of inducers is routinely employed to estimate the extent of tau polymerization, assess the effects of the modification of tau, and evaluate the effects of inhibitory compounds (*7*, *11*, *20*−*22*, *28*), our observations indicate that tau does not exhibit a true critical concentration for polymerization in the presence of inducer molecules.

Kinetics of Tau Polymerization Is Not Consistent with a Nucleation−*Elongation Mechanism*. The kinetics of a nucleation−elongation polymerization reaction has the general features of a lag phase, followed by an increase in polymerization to an apparent steady state. The analysis of the kinetics of polymerization in the presence of inducers is best fit by a single phase exponential association equation, without a lag phase due to nucleation that would indicate a critical concentration for polymerization. The $t_{1/2}$ for the polymerization process does not change with increasing protein concentrations but is rather affected only by the change in the inducer to protein ratio. Additionally, fitting the kinetic data to established models for polymerization indicates that the size of the nucleus for the ARA induced polymerization reaction is zero, indicating that there is no thermodynamic barrier for the nucleation of polymerization in the presence of this inducer. Therefore, our kinetic analysis indicates that tau polymerization in the presence of inducers does not follow the hallmarks of a nucleation−elongation reaction.

Concentration of Inducer Molecules Can Alter Tau Filament Morphology. The amount of tau polymerization observed was dependent on the concentration of inducer molecules (Figure 2). At low concentrations, the inducers limit the amount of polymerization because the addition of more inducer molecules results in greater protein polymerization. There is a peak in protein polymerization at an optimal ratio, and inducer concentrations greater than this optimum inhibit the reaction (Figure 2). In the inhibitory regime, the morphology of the filaments is also altered, resulting in smaller oligomers of tau that do not have the axial ratio that would indicate they are truly fibrillar (Figure 4). It has been suggested that these structures are intermediates in the polymerization process (*8*). However, our results indicate that these structures are generated as a result of high inducer concentrations rather than as an intermediate in the formation of longer fibrils. This conclusion is supported by the polymerization of tau into long fibrils even at very low protein concentrations when the inducer concentration is also kept low (Figure 5). The smaller oligomers generated at high inducer concentrations are instead the end product of a second polymerization pathway in which there is a great deal of nucleation but little elongation. This is of particular interest because similar structures, termed granular tau oligomers, have been detected in early stages of Alzheimer's disease (*29*). It has also been suggested that these oligomers likely represent a more toxic form of amlyoidogenic proteins in vivo (*30*). It is therefore possible that the specific cellular conditions and the availability of inducer molecules could alter the morphology and perhaps toxicity of tau filaments in vivo.

Inducers Act as Allosteric Regulators of Tau Polymerization. In several protein polymerization systems, including actin, the classic nucleation−elongation mechanism can be altered by the addition of small molecules such as Mg^{2+} that allosterically regulate polymerization. In these systems, the small molecules interact with the proteins and change their conformation such that the proteins then have a higher affinity for one another and the polymerized state, although they do not need to remain bound after polymerization has

been initiated (*12*). The general features of this regulation are (1) the lowering of the concentration of the protein required for polymerization in the presence of the regulatory molecules, (2) the dependence of the required concentration for protein polymerization on the concentration of regulatory molecules, and (3) a conformational change that accompanies the increased propensity for polymerization. ARA and heparin lower the concentration of protein required for polymerization, and this concentration of protein required depends on the concentration of inducer. A change in conformation can also be detected in the presence of inducers by the formation of β-structure in tau and may occur prior to the formation of tau filaments (*7*, *31*, *32*). Additionally, tau polymerized in the presence of ARA adopts a conformation that is recognized by the conformationally sensitive antibody Alz50 with an approximately 14-fold increase in affinity over that of the monomer (*9*). These results strongly suggest that ARA and heparin are acting allosterically to regulate the polymerization of tau. However, the levels of ARA and heparin binding to polymerized tau filaments are very low. This has been interpreted as ARA and heparin serving only as sources of nucleation and that they are not incorporated into the core of the filaments (*16*, *26*). If, however, ARA and heparin are serving as allosteric regulators of tau polymerization, it is not a requirement that they remain bound after the initiation of polymerization (*12*), which could provide an alternative explanation for their low degree of binding and is consistent with an allosteric regulation of tau polymerization. It should be noted that heparin molecules can differ by polymer length, which could affect the stochiometry of binding and optimal inducer conditions. Likewise, ARA has been shown to be affected by oxidation (*33*), which could also affect the stoichiometry of binding and optimal inducer conditions.

Physiological Relevance. Although it not known whether a physiological inducer of tau polymerization exists in AD or other related neurodegernative disorders, a strong case can be made for the potential involvement of ARA and/or heparin in this process. The levels of free cytoplasmic ARA are quite low in the normal brain where they are thought to play a role in normal maintenance and signaling in neurons. However, the level of cytoplasmic free fatty acids can become highly elevated under certain circumstances such as ischemia (*34*). In AD, there is an increase in the activity of cytoplasmic phospholipase$_2$, generating a metabolic cascade resulting in increased levels of fatty acids and fatty acid metabolites (*34*). The amounts of ARA derived isoprostanes and docasahexanoic derived neuroprostanes are elevated in AD (*35*, *36*), and conditions similar to those used to generate these species from free fatty acids in vitro (*37*) have been shown to enhance the ARA induction of tau polymerization in vitro (*33*). Other lipid metabolites such as 4-hydroxynonenal have also been shown to be elevated in AD and influence tau polymerization in vitro (*38*−*41*). Glycosaminoglycans such as heparin sulfate have been shown to be associated with neurofibrillary tangle pathology in AD, indicating a potential role for these molecules in the pathogenic process (*42*, *43*).

Despite the strong evidence for ARA and heparin as inducer molecules in the fibrilization of tau in AD described above, it is still not clear that these molecules are involved. It is possible that the observed hyperphosphorylation of tau in AD alone is sufficient to drive its aggregation (*44*, *45*) without the need for inducer molecules. An alternative explanation for the difficulty in identifying inducer molecules in AD is suggested by our current research. Our data strongly suggest that ARA and heparin are acting as allosteric regulators of tau polymerization. In many cases, such as the polymerization of actin, the allosteric regulator can be removed without disrupting the structure of the polymer (*46*). It is possible that once polymerization has been initiated by an allosteric regulator in AD, it is no longer required for the stability of the polymer and does not remain bound.

Conclusions. Our data indicate that ARA and heparin are allosteric effectors of tau polymerization and that polymerization is inhibited by high concentrations of inducer. These data indicate that even low levels of inducer reduce the protein concentration required for tau polymerization. High levels of inducer antagonize the process and result in the formation of short polymers, which may be more toxic than longer fibrils. Importantly, our data indicate that tau does not follow a true nucleation−elongation pathway for polymerization in the presence of inducer molecules. Instead, the critical concentration for polymerization in the presence of tau as documented previously (*7*, *11*, *20*−*22*, *28*) is more likely due to the limitations of the detection of filament formation. The current results indicate that the inducers are acting as allosteric modulators, both as activators at low concentrations and inhibitors at high concentrations.

ACKNOWLEDGMENT

We thank Dr. Audrey Lamb for the critical reading of the manuscript during its preparation.

REFERENCES

1. Lee, V. M., Goedert, M., and Trojanowski, J. Q. (2001) Neurodegenerative tauopathies, *Annu. Rev. Neurosci. 24*, 1121−1159.
2. Sergeant, N., Delacourte, A., and Buee, L. (2005) Tau protein as a differential biomarker of tauopathies, *Biochim. Biophys. Acta 1739*, 179−197.
3. Gamblin, T. C., Berry, R. W., and Binder, L. I. (2003) Modeling tau polymerization in vitro: a review and synthesis, *Biochemistry 42*, 15009−15017.
4. Kuret, J., Chirita, C. N., Congdon, E. E., Kannanayakal, T., Li, G., Necula, M., Yin, H., and Zhong, Q. (2005) Pathways of tau fibrillization, *Biochim. Biophys. Acta 1739*, 167−178.
5. Barghorn, S., and Mandelkow, E. (2002) Toward a unified scheme for the aggregation of tau into Alzheimer paired helical filaments, *Biochemistry 41*, 14885−14896.
6. Friedhoff, P., von Bergen, M., Mandelkow, E., and Davies, P. (1998) A nucleated assembly mechanism of alzheimer paired helical filaments, *Proc. Natl. Acad. Sci. U.S.A. 95*, 15712−15717.
7. Chirita, C. N., Congdon, E. E., Yin, H., and Kuret, J. (2005) Triggers of full-length tau aggregation: a role for partially folded intermediates, *Biochemistry 44*, 5862−5872.
8. Chirita, C. N., and Kuret, J. (2004) Evidence for an intermediate in tau filament formation, *Biochemistry 43*, 1704−1714.
9. King, M. E., Ahuja, V., Binder, L. I., and Kuret, J. (1999) Ligand-dependent tau filament formation: Implications for Alzheimer's disease progression, *Biochemistry 38*, 14851−14859.
10. Friedhoff, P., Schneider, A., Mandelkow, E. M., and Mandelkow, E. (1998) Rapid assembly of Alzheimer-like paired helical filaments from microtubule-associated protein tau monitored by fluorescence in solution, *Biochemistry 37*, 10223−10230.
11. Gamblin, T. C., King, M. E., Dawson, H., Vitek, M. P., Kuret, J., Berry, R. W., and Binder, L. I. (2000) In vitro polymerization of tau protein monitored by laser light scattering: method and application to the study of FTDP-17 mutants, *Biochemistry 39*, 6136−6144.
12. Oosawa, F., and Asakura, S. (1975) *Thermodynamics of the Polymerization of Protein*, Academic Press, London.

13. Rankin, C. A., Sun, Q., and Gamblin, T. C. (2005) Pseudophosphorylation of tau at Ser202 and Thr205 affects tau filament formation, *Brain Res. Mol. Brain. Res. 138*, 84−93.
14. DeTure, M., Granger, B., Grover, A., Hutton, M., and Yen, S. H. (2006) Evidence for independent mechanisms and a multiple-hit model of tau assembly, *Biochem. Biophys. Res. Commun. 339*, 858−864.
15. Horowitz, P. M., Lapointe, N., Guillozet-Bongaarts, A. L., Berry, R. W., and Binder, L. I. (2006) N-terminal fragments of tau inhibit full-length tau polymerization in vitro, *Biochemistry 45*, 12859−12866.
16. Chirita, C. N., Necula, M., and Kuret, J. (2003) Anionic micelles and vesicles induce tau fibrillization in vitro, *J. Biol. Chem. 278*, 25644−25650.
17. Necula, M., and Kuret, J. (2004) A static laser light scattering assay for surfactant-induced tau fibrillization, *Anal. Biochem. 333*, 205−215.
18. von Bergen, M., Friedhoff, P., Biernat, J., Heberle, J., and Mandelkow, E. (2000) Assembly of tau protein into Alzheimer paired helical filaments depends on a local sequence motif (306VQIVYK311) forming beta structure, *Proc. Natl. Acad. Sci. U.S.A. 97*, 5129−5134.
19. Wille, H., Drewes, G., Biernat, J., Mandelkow, E. M., and Mandelkow, E. (1992) Alzheimer-like paired helical filaments and antiparallel dimers formed from microtubule-associated protein tau in vitro, *J. Cell Biol. 118*, 573−584.
20. Necula, M., Chirita, C. N., and Kuret, J. (2005) Cyanine dye N744 inhibits tau fibrillization by blocking filament extension: implications for the treatment of tauopathic neurodegenerative diseases, *Biochemistry 44*, 10227−10237.
21. Necula, M., and Kuret, J. (2004) Pseudophosphorylation and glycation of tau protein enhance but do not trigger fibrillization in vitro, *J. Biol. Chem. 279*, 49694−49703.
22. Yin, H., and Kuret, J. (2006) C-terminal truncation modulates both nucleation and extension phases of tau fibrillization, *FEBS Lett. 580*, 211−215.
23. Berne, B. J. (1974) Interpretation of the light scattering from long rods, *J. Mol. Biol. 89*, 755−758.
24. Santa-Maria, I., Perez, M., Hernandez, F., Avila, J., and Moreno, F. J. (2006) Characteristics of the binding of thioflavin S to tau paired helical filaments, *J. Alzheimer's. Dis. 9*, 279−285.
25. Tobacman, L. S., and Korn, E. D. (1983) The kinetics of actin nucleation and polymerization, *J. Biol. Chem. 258*, 3207−3214.
26. von Bergen, M., Barghorn, S., Muller, S. A., Pickhardt, M., Biernat, J., Mandelkow, E. M., Davies, P., Aebi, U., and Mandelkow, E. (2006) The core of tau-paired helical filaments studied by scanning transmission electron microscopy and limited proteolysis, *Biochemistry 45*, 6446−6457.
27. Ko, L. W., DeTure, M., Sahara, N., Chihab, R., Vega, I. E., and Yen, S. H. (2005) Recent advances in experimental modeling of the assembly of tau filaments, *Biochim. Biophys. Acta 1739*, 125−139.
28. Reynolds, M. R., Berry, R. W., and Binder, L. I. (2005) Site-specific nitration and oxidative dityrosine bridging of the tau protein by peroxynitrite: implications for Alzheimer's disease, *Biochemistry 44*, 1690−1700.
29. Maeda, S., Sahara, N., Saito, Y., Murayama, S., Ikai, A., and Takashima, A. (2006) Increased levels of granular tau oligomers: an early sign of brain aging and Alzheimer's disease, *Neurosci. Res. 54*, 197−201.
30. Glabe, C. G. (2006) Common mechanisms of amyloid oligomer pathogenesis in degenerative disease, *Neurobiol. Aging 27*, 570−575.
31. von Bergen, M., Barghorn, S., Biernat, J., Mandelkow, E. M., and Mandelkow, E. (2005) Tau aggregation is driven by a transition from random coil to beta sheet structure, *Biochim. Biophys. Acta 1739*, 158−166.
32. Barghorn, S., Davies, P., and Mandelkow, E. (2004) Tau paired helical filaments from Alzheimer's disease brain and assembled in vitro are based on beta-structure in the core domain, *Biochemistry 43*, 1694−1703.
33. Gamblin, T. C., King, M. E., Kuret, J., Berry, R. W., and Binder, L. I. (2000) Oxidative regulation of fatty acid-induced tau polymerization, *Biochemistry 39*, 14203−14210.
34. Farooqui, A. A., and Horrocks, L. A. (2006) Phospholipase A2-generated lipid mediators in the brain: the good, the bad, and the ugly, *Neuroscientist 12*, 245−260.
35. Pratico, D., V, M. Y. L., Trojanowski, J. Q., Rokach, J., and Fitzgerald, G. A. (1998) Increased F2-isoprostanes in Alzheimer's disease: evidence for enhanced lipid peroxidation in vivo, *FASEB J. 12*, 1777−1783.
36. Reich, E. E., Markesbery, W. R., Roberts, L. J., II, Swift, L. L., Morrow, J. D., and Montine, T. J. (2001) Brain regional quantification of F-ring and D-/E-ring isoprostanes and neuroprostanes in Alzheimer's disease, *Am. J. Pathol. 158*, 293−297.
37. Roberts, L. J., II, Montine, T. J., Markesbery, W. R., Tapper, A. R., Hardy, P., Chemtob, S., Dettbarn, W. D., and Morrow, J. D. (1998) Formation of isoprostane-like compounds (neuroprostanes) in vivo from docosahexaenoic acid, *J. Biol. Chem. 273*, 13605−13612.
38. Markesbery, W. R., and Carney, J. M. (1999) Oxidative alterations in Alzheimer's disease, *Brain Pathol. 9*, 133−146.
39. Montine, K. S., Kim, P. J., Olson, S. J., Markesbery, W. R., and Montine, T. J. (1997) 4-Hydroxy-2-nonenal pyrrole adducts in human neurodegenerative disease, *J. Neuropathol. Exp. Neurol. 56*, 866−871.
40. Perez, M., Hernandez, F., Gomez-Ramos, A., Smith, M., Perry, G., and Avila, J. (2002) Formation of aberrant phosphotau fibrillar polymers in neural cultured cells, *Eur. J. Biochem. 269*, 1484−1489.
41. Santa-Maria, I., Hernandez, F., Martin, C. P., Avila, J., and Moreno, F. J. (2004) Quinones facilitate the self-assembly of the phosphorylated tubulin binding region of tau into fibrillar polymers, *Biochemistry 43*, 2888−2897.
42. Diaz-Nido, J., Wandosell, F., and Avila, J. (2002) Glycosaminoglycans and beta-amyloid, prion and tau peptides in neurodegenerative diseases, *Peptides 23*, 1323−1332.
43. Su, J. H., Cummings, B. J., and Cotman, C. W. (1992) Localization of heparan sulfate glycosaminoglycan and proteoglycan core protein in aged brain and Alzheimer's disease, *Neuroscience 51*, 801−813.
44. Alonso, A., Zaidi, T., Novak, M., Grundke-Iqbal, I., and Iqbal, K. (2001) Hyperphosphorylation induces self-assembly of tau into tangles of paired helical filaments/straight filaments, *Proc. Natl. Acad. Sci. U.S.A. 98*, 6923−6928.
45. Alonso, A. C., Grundke-Iqbal, I., and Iqbal, K. (1996) Alzheimer's disease hyperphosphorylated tau sequesters normal tau into tangles of filaments and disassembles microtubules, *Nat. Med. 2*, 783−787.
46. Kasai, M., and Oosawa, F. (1963) Removal of nucleotides from F-actin, *Biochim. Biophys. Acta 75*, 223−233.

BI700403A